

A comparison of leak compensation during pediatric non-invasive positive pressure ventilation; a lung model study

Jun Oto, M.D., PhD, Research fellow Respiratory Care Services, Massachusetts General Hospital

E-mail address: JOTO@PARTNERS.ORG

Christopher T. Chenelle, B.A., Respiratory Care Services, Massachusetts General Hospital

E-mail address: CCHENELLE@PARTNERS.ORG

Andrew D. Marchese, B.S., Respiratory Care Services, Massachusetts General Hospital

E-mail address: ANDY@CSAIL.MIT.EDU

Robert M Kacmarek PhD, RRT, Respiratory Care Services, Massachusetts General Hospital

E-mail address: RKACMAREK@PARTNERS.ORG

Address correspondence to:

Robert M Kacmarek PhD, RRT, Respiratory Care Services, Massachusetts General Hospital

E-mail address: RKACMAREK@PARTNERS.ORG

55 Fruit street, Boston, MA, 02114

Tel: 617-724-4490, Fax: 617-724-4495

Financial support: Funded in part by COVIDIEN, Inc., 6135 Gunbarrel Avenue, Boulder, CO 80301

Conflict of interest: Robert M Kacmarek: Maquet Inc received honorarium for lecturing, received research grant from COVIDIEN, Consultant for COVIDIEN. All other authors have no conflict of interest.

Keywords: leak compensation, pediatric non-invasive positive pressure ventilation, acute care ventilator

Abstract

Background: Ventilators used for non-invasive positive pressure ventilation (NIV) must be able to synchronize in the presence of system leaks. We compared the ability of 7 ICU ventilators and 3 dedicated NIV ventilators to compensate for leaks during pediatric NIV.

Method: Using a lung simulator, the Maquet Servo-*i*, the Dräger V500, the Dräger Carina, the Covidien PB840, the Respironics V60, the Respironics Vision, the General Electric Engström Carestation, the CareFusion Avea, the Hamilton C3 and the Hamilton G5 were compared during increasing (n=6) and decreasing leaks (n=6). Leak levels used were: BL (baseline of 2–3 L/min), L1 (5–6 L/min), L2 (9–10 L/min) and L3 (19–20 L/min). Three patient sizes (10, 20, and 30 kg) with three different lung mechanics (normal, obstructive, and restrictive models) were simulated by the ASL5000 lung simulator. Ventilator settings were non-invasive ventilation mode, pressure support 10 cmH₂O and PEEP 5 cmH₂O. The rate of synchronization (synchronized cycles/total simulated respirations) was recorded for each ventilator for each leak scenario. Synchronization was defined as triggering without auto-triggering, miss-triggering, delayed cycling or premature cycling.

Results: The mean rate of synchronization across all ventilators was 68±27% (range: 23%–96%) and marked differences existed between ventilators ($p < 0.001$). Significant differences in the rate of synchronization were observed between the 10 kg (mean: 57±30%; range: 17%–93%), the 20 kg (69±30%; 25%–98%) and the 30 kg models (77±22%; 28%–97%) ($p < 0.001$). The synchronization rate for the obstructive model (60±30%; 9%–94%) was significantly different from the normal model (71±29%;

18%–98%) and the restrictive model ($72 \pm 28\%$; 23%–98%) ($p < 0.001$). The PB840 and the C3 had synchronization rates over 90% with all body weights, all lung mechanic profiles and all leak levels.

Conclusions: Leak compensation in NPPV for pediatric use can partially compensate for leaks, but varies widely among ventilators, patient weights, and lung mechanics.

Introduction

Noninvasive positive pressure ventilation (NIV) has been used as a treatment for acute and chronic respiratory failure in adults¹ and in children². In adult patients, high-level evidence supports the use of NIV in cardiogenic pulmonary edema, exacerbation of chronic obstructive pulmonary disease, neuromuscular disorders and respiratory distress in the immuno-compromised patient¹. Although the application of NIV for pediatric patients is less established than for adult patients, NIV is considered as an acceptable form of ventilation in children with severe obstructive sleep apnea syndrome³, postextubation respiratory failure^{4, 5}, immuno-compromised acute respiratory failure⁶, and chronic respiratory failures such as neuromuscular disease⁷ or cystic fibrosis⁸.

While NIV theoretically allows for respiratory system muscle unloading, alveolar recruitment, oxygenation, and CO₂ washout, patient-ventilator asynchrony is a major issue leading to NIV treatment failure^{9, 10}. There are many ventilators available for NIV for children, but particularly in small children, triggering and cycling problems occur frequently¹⁰. Pediatric patients with respiratory failure may develop an extreme breathing pattern with higher respiratory rates and small tidal volumes, leading to an inability to achieve sufficient inspiratory flow to trigger a breath¹¹. In addition, gas leaks around the face mask lead to auto-triggering, miss-triggering and delayed cycling^{11, 12}. Essouri et al. reported that triggering asynchrony occurred in 33% of patients studied with auto-triggering and miss-triggering occurring in up to 38% and 20% of total patient breaths, respectively⁹. Fauroux et al. performed a bench study to evaluate the response of 17 home

care ventilators on six pediatric profiles¹⁰. No ventilator was able to adequately ventilate the six pediatric profiles, mainly due to insufficient trigger sensitivity¹⁰.

Recently, manufacturers have implemented leak compensation on the latest acute care ventilators to compensate for and better manage leaks. In adult settings, some bench studies assessing leak compensation have shown improved triggering and cycling synchronization but with wide variation among ventilators^{13, 14}. To the best of our knowledge, there have been no assessments of leak compensation during pediatric NIV. The goal of this study was to evaluate the ability of acute care ventilators to prevent triggering and cycling asynchrony in the presence of leaks during pediatric NIV.

Methods

Seven ICU ventilators (Maquet Servo-*i*, Covidien PB840, Hamilton C3, Hamilton G5, General Electric Engström Carestation, Dräger V500, CareFusion Avea) and three dedicated NIV ventilators (Respironics V60, Respironics BiPAP Vision, Dräger Carina) were compared using the ASL5000 lung model (IngMar Medical; Pittsburgh, PA) with increasing and decreasing system leaks (Table 1). The ASL5000 is a computerized lung simulator consisting of a piston moving inside a cylinder¹⁵. The ASL5000 incorporates a series of three user-controlled leaks with a simulator bypass and leak valve module (SBLVM: IngMar Medical; Pittsburgh, PA). Gas leak was created at the airway opening of the lung simulator by three different orifice sizes and is nonlinearly related to pressure and flow. Compliance, resistance, and the inspiratory muscle pressure profile (negative pressure created by respiratory muscles) are set by the user. Each ventilator was connected to the lung simulator by the manufacturer's standard circuit, if available, or a standard pediatric corrugated circuit (Hudson; Temecula, CA). All of the ventilators were studied with a dry circuit; humidifiers and heat and moisture exchanger were removed.

Study setup (ASL5000 interface and mannequin)

The ASL5000 was used to simulate three pediatric models with different lung sizes based on weight (10, 20, and 30 kg) (Figure 1). We modeled lung diseases by adjusting airway resistance, and lung compliance of the model corresponding to 1) a normal lung model, 2) an obstructive lung model and 3) a restrictive lung model. The inspiratory time of

the simulator, the maximum inspiratory pressure drop, the pressure drop generated 100 ms after the onset of an occluded inspiratory effort ($P_{0.1}$), and the respiratory rate in each model are summarized in Table 2. We chose these lung model settings either by referenced values, pediatric and adult model studies, or by measurements that we felt has been commonly observed in the clinical setting for mechanically ventilated patients of these sizes^{13, 16}. In pressure support ventilation, the set peak inspiratory pressure (PIP)-generated tidal volume was 7–10 ml/kg in the normal model in each body weight with baseline leak. PIP/PEEP was set at 15/5 cm H₂O as described below. Two different sizes of mannequin heads (bigger for the 30 kg model and smaller for the 20 kg and 10 kg models) were used to simulate the patient-mask interface. Endotracheal tubes fitted into the mouth and nostrils directed gas coming from a facemask to the simulator (Figure 1). These nasal and oral tubes met in a common airway leading to the SBLVM; the SBLVM then lead to the ASL5000. An oronasal facemask (PerformaTrack SE; Respironics Inc; Murrysville, PA) for 30 kg model was affixed to the head of the mannequin with standard straps. A nasal mask (Contour DeluxeTM, Respironics Inc; Murrysville, PA) was used as an oronasal mask for both the 20 kg and 10 kg models. A baseline leak of approximately 2 to 3 L/min (baseline leak: B) at a mean airway pressure of 5 cmH₂O was established prior to each evaluation. The SBLVM was set to established leak flows of 5 to 6 L/min (leak level 1: L1), 9 to 10 L/min (L2) and 19 to 20 L/min (L3) at a mean airway pressure of 5 cmH₂O. All combinations of increasing leak changes (B→L1, B→L2, B→L3, L1→L2, L1→L3, L2→L3: 6 in total) and of decreasing leak changes (L3→L2, L3→L1, L3→B, L2→L1, L2→B, L1→B: 6 in total) were evaluated.

Ventilator setup

During ventilator assessment, all ventilators were set in the NIV mode, as follows: pressure support mode; inspiratory pressure, 10 cm H₂O; positive end-expiratory pressure, 5 cmH₂O; respiratory rate, 4 breaths/min; leak compensation activated. Trigger sensitivity, when adjustable, was set to be as sensitive as possible while avoiding auto-triggering at baseline leak; inspiratory rise time, when adjustable, was set to the most rapid setting while avoiding overshooting of the set peak pressure. Termination criteria, when adjustable, were set at 25% of peak flow. If delayed cycling occurred in the presence of leak, the termination criteria were adjusted to avoid the delayed cycling and the data was collected with these same settings through the study. The “normal” cycling setting with the dedicated NIV ventilators resulted in delayed cycling at baseline leak. In the Carina, triggering sensitivity and termination criteria were set at “sensitive”. In the V60, termination criteria were set to avoid delayed cycling. With the Vision neither triggering nor cycling is adjustable. The maximum duration of inspiration was set to 1.5 sec if available.

Data collection, variables and evaluation

All combinations of increasing or decreasing leaks created by the SBLVM were sequentially added to the system. After each change in leak level, we collected 2 minutes of data. The following variables were analyzed: the rate of synchronization, expressed as a percentage and calculated as follows: the rate of synchronization (%)= (synchronized cycles/total simulated respiratory rate during 2 min)×100, auto-triggering: the rate of

auto-triggering (%) = (auto-triggered cycles/ total simulated respiratory rate during 2 min) $\times 100$ and miss-triggering: the rate of miss-triggering (%) = (miss-triggered cycles/ total simulated respiratory rate during 2 min) $\times 100$. Synchronization was defined as triggering without auto-triggering, miss-triggering, delayed cycling or premature cycling. In this evaluation, ventilators that achieved over 90% synchronization rate were considered appropriate for pediatric NIV¹⁶. Delayed cycling was defined by a cycling delay time (time from the end of the inspiratory effort of the simulator to the moment the ventilator cycled from inspiration to expiration) greater than two times the inspiratory time of the simulator¹⁶. Premature cycling was defined by an inspiratory time of the ventilator less than half of the inspiratory time of the simulator¹⁶. In addition, the following variables were evaluated: triggering delay time, the time from the beginning of the inspiratory effort of the lung simulator to the maximum negative airway pressure deflection needed to trigger the ventilator and delivered tidal volume. Since a triggering delay time of approximately 15 % of the inspiratory time was considered an acceptable range in adult model studies^{13, 17}, we considered triggering delay times below 70, 85, and 105 ms for the 10, 20, and 30 kg models, respectively, as acceptable values.

Statistical analysis

After stabilization, 2 minutes of data were collected and 5 consecutive breaths were analyzed for cycling time, triggering delay time, and delivered tidal volume. Offline analysis of each breath was performed by the ASL5000 software (Labview; National Instruments; Austin, TX). The results were presented as the mean \pm SD or median (range)

depending on the parametric or non-parametric nature of the data distribution. ANOVA and Bonferroni test for multiple comparisons were used for overall comparisons between ventilators, for comparisons of lung mechanics within each ventilator and for comparisons of each body weight and levels of leak within each ventilator and across ventilators.

Statistical analysis was done with a statistical software package (PASW Statistic 18; SPSS; Chicago, IL). A $p < 0.05$ was considered significant, however, only those comparisons that were both statistically significant and differing by at least 10% are discussed.

Results

Synchronization

The mean rate of synchronization across all ventilators was $68 \pm 27\%$ (range: 23%–96%). Significant differences in the rate of synchronization were observed between the 10 kg (mean: $57 \pm 30\%$; range: 17%–93%), the 20 kg ($69 \pm 30\%$; 25%–98%) and the 30 kg models ($77 \pm 22\%$; 28%–97%) ($p < 0.001$) (Figure 2). The rate of synchronization of the obstructive model ($60 \pm 30\%$; 9%–94%) was significantly different from the normal model ($71 \pm 29\%$; 18%–98%) and restrictive model ($72 \pm 28\%$; 23%–98%) ($p < 0.001$) (Figure 2). As leak increased, the rate of synchronization decreased (B: mean $88 \pm 9\%$; range 68%–100%, L1: $69 \pm 32\%$; 6%–99%, L2: $64 \pm 35\%$; 0%–97%, L3: $51 \pm 39\%$; 0%–94%) (Figure 2). The rate of synchronization was lower and auto-triggering was higher for increasing leaks than for decreasing leaks ($p < 0.001$) (Suppl. Figure 1).

Comparison among ventilators:

The PB840 and the C3 synchronized over 90% with all body weights, all lung mechanics profiles and all leak levels (Figure 2). In the 10 kg model, the PB840 and the C3 synchronized above 90% overall across the lung mechanics profiles, but no ventilators synchronized over 90% in the obstructive model alone (the PB840: 87%, the C3: 89%). In the 20 kg model, the Servo *i*, the PB840, the C3, the Carina, and the V60 achieved over 90% synchronization (Figure 2). In the 30 kg model, the same ventilators as 20 kg model, except for the V60, achieved over 90% of synchronization (Figure 2).

Type of asynchronization:

The Servo *i*, the C3, the G5 and the Avea tended to prolong inspiratory time at cycling criteria of 25% of peak inspiratory flow. Thus, these ventilators were managed using the cycling criteria at 45–60% of peak inspiratory flow (Suppl. Figure 2A). On the other hand, the PB840, the Carestation, and the V500 did not show the prolonged inspiratory time at 25% of peak inspiratory flow, but values of the cycling criteria over 25% induced shorter inspiratory times than the lung model (Suppl. Figure 2B). Among all ventilators, auto-triggering occurred in 54% of total asynchronies, miss-triggering in 37% and delayed cycling in 9%. Except for the Vision, the rate of delayed cycling was under 1% of the total simulated respiratory rate. Premature cycling was seen only in the PB840 (0.02% of total simulated respiratory rate). The causes of asynchronies are summarized in Figure 3.

In the obstructive model, auto-triggering was less frequent than in the normal and restrictive models ($p < 0.001$) (Figure 4). As leak increased, the rate of auto-triggering increased ($p < 0.001$) (Figure 4). In the obstructive model, miss-triggering was more frequent than in the normal and restrictive models ($p < 0.001$) (Figure 5). As body weight decreased, miss-triggering increased ($p < 0.001$) (Figure 5).

Triggering delay time:

The mean triggering delay time was longer in the obstructive model (107 ± 20 ms) than in the normal (87 ± 21 ms) and restrictive models (81 ± 18 ms) ($p < 0.001$). As leak

increased, the mean triggering delay time increased (B: 87 ± 18 ms, L1: 88 ± 20 ms, L2: 92 ± 20 ms, L3: 105 ± 23 ms, $p < 0.001$). The Servo *i* and the Vision showed mean triggering delay times over 100 ms (Servo *i*: 116 ± 15 ms, Vision: 107 ± 8 ms) (Suppl. Table 1). In 10 kg model, all ventilators showed triggering delay times over the acceptable range (< 70 ms), except during baseline leak.

Tidal volume:

Significant differences in tidal volume were observed between the 10 kg (median: 70 ± 15 ml), the 20 kg (126 ± 27 ml) and the 30 kg models (187 ± 46 ml) ($p < 0.001$) (Suppl. Table 1). The mean tidal volume was larger in the normal model (169 ± 63 ml) than in the obstructive (123 ± 45 ml) and restrictive models (112 ± 42 ml) ($p < 0.001$). As leak increased, tidal volume decreased (B: median 139 ± 58 ml, L1: 136 ± 57 ml, L2: 130 ± 54 ml, L3: 115 ± 50 ml, $p < 0.001$) (Suppl. Table 1).

Discussion

The main findings of this study are as follows: 1) smaller patient size, obstructive lung mechanics, and higher system leaks decrease the ability of mechanical ventilators to synchronize during simulated pediatric NIV; 2) triggering asynchrony was more common than cycling asynchrony; 3) auto-triggering increased with larger system leak and decreased with the obstructive lung model; 4) miss-triggering increased with smaller patient size and with the obstructive lung model; 5) ventilators performed better during decreasing than increasing leak; 6) there were wide variations in ability to synchronize between ventilators. The PB840 and the C3 had synchronization rates over 90% with all body weights, lung mechanic profiles and leak levels. This is the first bench study to evaluate the performance of leak compensation among acute care ventilators for nine different pediatric patient profiles (three patient sizes with three different lung mechanics) in the presence of three different leak levels.

As patient size increased, the ventilators showed better synchronization with the lung simulator. In the 10 kg model, the inspiratory efforts were lower, leading to a reduction in the ability of the ventilators to detect the onset of inspiration and expiration. In addition, the airway resistance was higher in the 10 kg model than the 20 kg and 30 kg models, which also impaired the triggering function and led to miss-triggering and delayed cycling. In this study, miss-triggering was more frequent with low body weight and obstructive lung model conditions. The limitations of bi-level pressure-targeted ventilators during NIV in small children are well documented in recent clinical⁹ and bench studies¹⁰. Essouri et al.

reported that all patients who were under 10 kg showed marked patient-ventilator asynchrony (ineffective inspiratory efforts ranging from 32% to 97% of inspiratory efforts), and 33% of patients over 10 kg also showed patient-ventilator asynchrony⁹. In a bench study, Fauroux et al. evaluated the performance of 17 home ventilators during NIV for different pediatric profiles and showed that none of these ventilators synchronized well with every patient profile and that the more sensitive a ventilator was to leaks, the less responsive it was to patient triggering efforts, especially in the smallest patient size¹⁰.

In the obstructive model, miss-triggering was more frequent than in the normal and restrictive models. Compared to the normal and restrictive models, the obstructive model showed increased triggering delay time. These results were consistent with those of previous reports^{16, 18}. This may be explained by the presence of a higher airway resistance, which impedes the transmission of respiratory efforts to the ventilator and requires larger efforts to reach the trigger threshold due to higher pressure gradients throughout the airway.

Ventilators performed better during decreasing than increasing leak scenarios. As system leak increases, the ventilators misinterpreted the resulting changes in flow as inspiratory efforts, leading to frequent auto-triggering. Vignaux et al. found that in patients showing auto-triggering, the magnitude of leak was higher than those not showing it. However, they found no correlation between leak volume and the severity of auto-triggering¹⁹. A possible reason for the difference is that our simulated leak levels had a wider range (from 3–4 L/min to 19–20 L/min) than the previous study¹⁹ (up to 6.1 L/min). Also, in our study, some ventilators could not synchronize in the presence of larger leaks, especially L2 (9–10 L/min) and L3 (19–20 L/min), mainly due to auto-triggering. Another

reason was that we tested 10 different ventilators. The frequency of auto-triggering depends on the ventilator performance as described in previous studies^{13, 14, 17, 20}. Auto-triggering was less frequent in the obstructive model than the normal or restrictive models and this concurs with previous reports²¹⁻²³.

Most acute care ventilators have cycling systems based on a preset flow threshold. System leak prevents the airflow from reaching the preset expiratory cycling flow, leading to a prolonged inspiratory time and patient-ventilator asynchrony⁸. This study showed that delayed cycling was not the main cause of patient-ventilator asynchrony in the presence of system leak, if the termination criteria were adjustable. However, appropriate cycling criteria seemed to be different between ventilators. Regarding the ICU ventilators, the Servo *i*, the C3, the G5 and the Avea tended to prolong inspiratory time at cycling criteria of 25% of peak inspiratory flow but cycled appropriately at 50–60% of peak inspiratory flow (Suppl. Figure 2A). On the other hand, in the PB840, the Carestation, and the V500, 25% of peak inspiratory flow was better than 50–60% in the restrictive model (Suppl. Figure 2B). With dedicated NIV ventilators, if the “normal” cycling setting was used, these three ventilators showed delayed cycling, especially in the normal and obstructive models. Dedicated NIV ventilators transition to exhalation primarily by what is referred to as a shape signal and tend to prolong inspiratory time compared with ICU ventilators. Adjustable sensitivity of the inspiratory and expiratory triggers is of great importance in both dedicated NIV ventilators and ICU ventilators for pediatric use. Because the Vision has a fixed inspiratory and expiratory flow-trigger, delayed cycling occurred frequently. In this case, it may be better to use time cycled criteria to avoid delayed cycling²⁴.

Our study indicates that the leak compensation on acute care ventilators can correct partially or completely for system leak interferences in pediatric lung simulators, but there was wide variation among ventilators. In general, the PB840, the C3 and the Carina achieved over 90% synchronization. Vignaux et al. performed a bench study of 8 ICU ventilators featuring leak compensation¹⁴. On most of the tested ventilators, leaks led to an increase in trigger delay and decrease in ability to reach the pressure target and delayed cycling. Similar to our findings, they found that the NIV mode partially or completely corrected for triggering and cycling delay, and there was marked variation among ventilators¹⁴. Since the manufacturers do not disclose the exact triggering and cycling algorithms for leak compensation, it is impossible to explain the wide variations in ability to synchronize among ventilators tested.

Regarding trigger delay, most ventilators, except for the Servo *i* and the Vision, showed triggering delay times lower than the predefined acceptable values in the 20 kg and 30 kg models. However, no ventilator achieved a triggering delay time lower than the predefined acceptable values in the 10 kg model. Because a prolonged trigger delay may lead to an increase of patient work of breathing and patient-ventilator asynchrony, further technical improvements are needed to insure appropriate application of NIV to pediatric patients under 10 kg.

The primary limitation of this study is that the study was not conducted on patients, raising the question of the extent that the findings may be clinically relevant. Although we used a sophisticated lung model, this is not the same as an actual patient's respiratory system. In clinical settings, respiratory rate, inspiratory time as well as $P_{0.1}$ and P_{\max} may be

different among patients with normal, obstructive, and restrictive lung mechanics. However, we mainly focused on the effects of different lung compliance, airway resistance and patients' sizes on the synchronization ability of ventilators. For children who required mechanical ventilation, Harikumar et al. measured a $P_{0.1}$ of -2.4 (range: -0.9 to -6.1) cm H_2O ²⁵. A breathing effort of -2.8 to -3.9 cm H_2O , the values we chose in this study, probably correspond to the median effort for pediatric patients who required mechanical ventilation. In addition, lung simulator studies assure that experimental conditions are the same for each ventilator evaluated. It is impossible, especially in pediatric patients, to control the level of the leak or maintain stable baseline conditions in clinical settings. Another limitation is that we tested only a limited range of leaks and ventilator settings. However, we chose these to represent the range of leak flows that are likely to be encountered in clinical settings during non-invasive ventilation. In addition, we were interested in evaluating the maximum capabilities of the ventilators tested.

In conclusion, leak readily leads to patient-ventilator asynchrony, especially in small pediatric patients. Clinicians should be careful to decrease leak as much as possible. All of the acute care ventilators tested can adequately synchronize with simulated ventilatory efforts at baseline, and some ventilators synchronize well with high-level leaks, but there are wide variations among ventilators. The performance of all ventilators was strongly affected by the patient profile, including body size and underlying lung mechanics. Clinicians should be aware of these differences when applying leak compensation during NIV, especially for children. Although the PB840 and the C3 showed better synchrony with triggering and cycling than other ventilators, the clinical significance of these differences is

unclear. Further studies are needed to determine the impact of different ventilators on the outcome of different groups of patients receiving NIV.

References

1. Hill NS, Brennan J, Garpestad E, Nava S. Noninvasive ventilation in acute respiratory failure. *Crit Care Med* 2007;35(10):2402-2407.
2. Calderini E, Chidini G, Pelosi P. What are the current indications for noninvasive ventilation in children? *Curr Opin Anesthesiol* 2010;23(3):368-374.
3. Marcus CL, Rosen G, Ward SL, Halbower AC, Sterni L, Lutz J, Standing PJ, Bolduc D, Gordon N. Adherence to and effectiveness of positive airway pressure therapy in children with obstructive sleep apnea. *Pediatrics* 2006;117(3):e442-e451.
4. Gupta P, Kuperstock JE, Hashmi S, Arnolde V, Gossett JM, Prodhan P, et al. Efficacy and predictors of success of noninvasive ventilation for prevention of extubation failure in critically ill children with heart disease. *Pediatr Cardiol* 2013;34(4):964-977.
5. Stucki P, Perez MH, Scalfaro P, de Halleux Q, Vermeulen F, Cotting J. Feasibility of non-invasive pressure support ventilation in infants with respiratory failure after extubation: a pilot study. *Intensive Care Med* 2009;35(9):1623-1627.
6. Piastra M, De Luca D, Pietrini D, Pulitanò S, D'Arrigo S, Mancino A, Conti G. Noninvasive pressure-support ventilation in immunocompromised children with ARDS: a feasibility study. *Intensive Care Med* 2009;35(8):1420-1427.
7. Mellies U, Ragette R, Dohna Schwake C, Boehm H, Voit T, Teschler H. Long-term noninvasive ventilation in children and adolescents with neuromuscular disorders. *Eur Respir J* 2003;22(4):631-636.
8. Fauroux B, Piquet J, Polkey MI, Isabey D, Clément A, Lofaso F. In vivo physiologic

- comparison of two ventilators used for domiciliary ventilation in children with cystic fibrosis. *Crit Care Med* 2001;29(11):2097-2105.
9. Essouri S, Durand P, Chevret L, Haas V, Perot C, Clement A, Devictor D, Fauroux B. Physiological effects of noninvasive positive ventilation during acute moderate hypercapnic respiratory insufficiency in children. *Intensive Care Med* 2008;34(12):2248-2255.
 10. Fauroux B, Leroux K, Desmarais G, Isabey D, Clément A, Lofaso F, Louis B. Performance of ventilators for noninvasive positive-pressure ventilation in children. *Eur Respir J* 2008;31(6):1300-1307.
 11. Teague WG. Non-invasive positive pressure ventilation: current status in paediatric patients. *Paediatr Respir Rev* 2005;6(1):52-60.
 12. Hess DR. Patient-ventilator interaction during noninvasive ventilation. *Respir Care* 2011;56(2):153-165.
 13. Ferreira JC, Chipman DW, Hill NS, Kacmarek RM. Bilevel vs. ICU ventilators providing noninvasive ventilation: effect of system leaks: a COPD lung model comparison. *Chest* 2009;136(2):448-456.
 14. Vignaux L, Tassaux D, Jolliet P. Performance of noninvasive ventilation modes on ICU ventilators during pressure support: a bench study. *Intensive Care Med* 2007;33(8):1444-1451.
 15. IngMar Medical. ASL5000 Active Servo Lung Computerized Breathing Simulator and Ventilator Test Instrument user's manual. Pittsburgh, PA: IngMar Medical, 2006
 16. Thille AW, Rodriguez P, Cabello B, Lellouche F, Brochard L. Patient-ventilator

- asynchrony during assisted mechanical ventilation. *Intensive Care Med* 2006;32(10):1515-1522
17. Carteaux G, Lyazidi A, Cordoba-Izquierdo A, Vignaux L, Jolliet P, Thille AW, Richard JCM, Brochard L. Patient-ventilator asynchrony during noninvasive ventilation: A bench and clinical study. *Chest* 2012;142(2):367-376.
 18. Chao DC, Scheinborn DJ, Stearn-Hassenpflug M. Patient-trigger asynchrony in prolonged mechanical ventilation. *Chest* 1997;112(6):1592-1599
 19. Vignaux L, Vargas F, Roeseler J, Tassaux D, Thille AW, Kossowsky MP, Brochard L, Jolliet P. Patient-ventilator asynchrony during non-invasive ventilation for acute respiratory failure: a multicenter study. *Intensive Care Med* 2009;35(5):840-846.
 20. Oto J, Chenelle CT, Marchese AD, Kacmarek RM. A comparison of leak compensation in acute care ventilators during non-invasive and invasive ventilation: a lung model study. *Respir Care* 2013[Epub ahead of print] doi:10.4187/respcare.02466
 21. Imanaka H, Nishimura M, Takeuchi M, Kimball WR, Yahagi N, Kumon K. Autotriggering caused by cardiogenic oscillation during flow-triggered mechanical ventilation. *Crit Care Med* 2000;28(2):402-407.
 22. Prinianakis G, Delmastro M, Carlucci A, Ceriana P, Nava S. Effect of varying the pressurization rate during noninvasive pressure support ventilation. *Eur Respir J* 2004;23(2):314-320
 23. Hill LL, Pearl RG. Flow triggering, pressure triggering, and autotriggering during mechanical ventilation. *Crit Care Med* 2000;28(2):579-581.
 24. Calderini E, Confalonieri M, Puccio PG, Francavilla N, Stella L, Gregoretti C.

Patient-ventilator asynchrony during noninvasive ventilation: the role of expiratory trigger. *Intensive Care Med* 1999;25(7):662-667.

25. Harikumar G, Moxham J, Greenough A, Rafferty GF. Measurement of maximal inspiratory pressure in ventilated children. *Pediatr Pulmonol* 2008;43(11):1085-1091.

Figure legends

Figure 1

Illustration of the experimental setup.

Different ventilators are connected to the mask on the head of the mannequin and deliver air to the ASL5000 lung simulator with the SBLVM during non-invasive ventilation.

SBLVM, simulator bypass and leak valve module

Figure 2

Synchronization rates among ventilators

Top left) Synchronization rates by body weight.

This figure shows the net percentage of synchronization of each ventilator for each bodyweight across all leak scenarios and lung conditions. Synchronization rates increased with bodyweight ($p < 0.001$).

Bottom left) Synchronization rates by lung conditions.

This figure shows the net percentage of synchronization of each ventilator for each lung condition across all leak scenarios and body weights. Synchronization rates were lower in the obstructive model than the normal and the restrictive models ($p < 0.001$).

Bottom right) Synchronization rates by leak level.

This figure shows the net percentage of synchronization of each ventilator for each leak level across all body weights and lung conditions. As leak increased, the rate of synchronization decreased ($p < 0.001$).

The histogram bars show mean values.

Figure 3

Causes of asynchrony among the ventilators.

This figure shows the relative contribution of each type of asynchrony (auto-triggering, missed-triggering and delayed cycling) as a percentage of total simulated breaths for each ventilator across all scenarios.

Premature cycling is not shown because it occurred only in the PB840 at a percentage of under 0.1% of simulated respirations.

The histogram bars show mean values.

Figure 4

Percentage of auto-triggering out of total simulated breaths among ventilators.

Top left) Auto-triggering by body weight.

This figure shows the rates of auto-triggering of each ventilator for each bodyweight across all leak scenarios and lung conditions. Auto-triggering rates were not associated with bodyweight ($p=0.1$).

Left bottom) Auto-triggering by lung conditions.

This figure shows the rate of auto-triggering of each ventilator for each lung condition across all leak scenarios and body weights. Auto-triggering was lower in the obstructive model than the normal and the restrictive models ($p < 0.001$).

Bottom Right) Auto-triggering by leak level.

This figure shows the rates of auto-triggering of each ventilator for each leak level across all body weights and lung conditions. As leak increased, the rate of auto-triggering increased ($p < 0.001$).

The histogram bars show mean values.

Figure 5

Percentage of miss-triggering out of total simulated breaths among ventilators.

Top left) Miss-triggering by body weight.

This figure shows the rates of miss-triggering of each ventilator for each bodyweight across all leak scenarios and lung conditions. Miss-triggering increases with decreased bodyweight ($p < 0.001$).

Bottom left) Miss-triggering by lung conditions.

This figure shows the rates of miss-triggering of each ventilator for each lung condition across all leak scenarios and body weight. Miss-triggering was higher in the obstructive model than the normal and the restrictive models ($p < 0.001$).

Bottom right) Miss-triggering by leak level.

This figure shows the rates of miss-triggering of each ventilator for each leak level across all body weights and lung conditions. Miss-triggering was not associated with leak level ($p=0.06$).

The histogram bars show mean values.

Table 1. Ventilator specification and evaluated with sensitivity, rise time and expiratory trigger setting

Ventilator	Software	Leak Compensation	Sensitivity	Rise time	E cycle
Servo i	V5.00.00	NIV:50 L/min	NA	0 ms	50%
PB840	4-070212-85-AG	NIV: 65 L/min	1 L/min	100%	25%
C3	1.0.0	No information	1 L/min	25 ms	50 – 60%
G5	2.1X	No information	1 L/min	25 ms	50 – 60%
V500	2.23	180 L/min	1 L/min	0 ms	25%
CareStation	5.0	No information	1 L/min	0 ms	25%
Avea	4.4	No information	1 L/min	1 (fastest)	45%
Carina	3.n	180 L/min	Sensitive	0.1 s	Sensitive
V60	PN 1076723 Auto-Track+	60 L/min	+5	1 (fastest)	Nor, Obst: +3 – +5 Rest: normal
Vision	13.4	60 L/min	NA	0.05 s	NA

IT sensitivity, inspiratory trigger sensitivity; E cycle, expiratory trigger setting (expressed as a percentage of inspiratory flow);

NA, not adjustable; NIV, non-invasive ventilation mode; Nor, normal model; Obst, obstructive model; Rest, restrictive model.

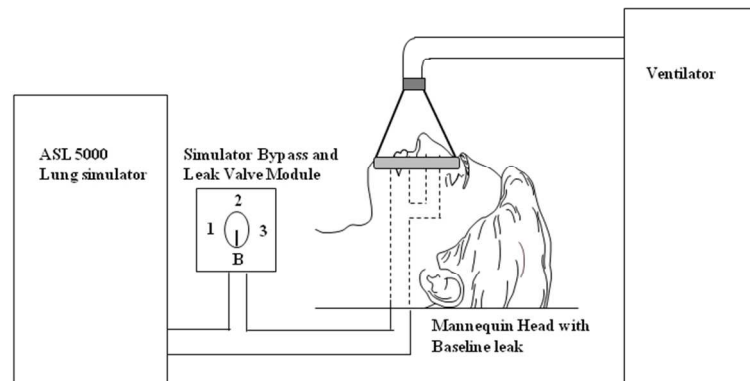
Table 2. Lung model settings

Models	Lung mechanics	Compliance (ml/cmH ₂ O)	Resistance (cmH ₂ O/L/s)	P _{0.1} (cmH ₂ O)	P _{max} (cmH ₂ O)	FRC (ml)	RR (/min)	I-time (s)
10 kg	Normal	10	25	-2.8	-4.0	300	30	0.46
	Obstructive	10	50	-2.8	-4.0	600	30	0.46
	Restrictive	5	25	-2.8	-4.0	150	30	0.46
20 kg	Normal	20	20	-3.3	-4.5	600	25	0.55
	Obstructive	20	40	-3.3	-4.5	1200	25	0.55
	Restrictive	10	20	-3.3	-4.5	300	25	0.55
30 kg	Normal	30	15	-3.9	-5.0	900	20	0.69
	Obstructive	30	30	-3.9	-5.0	1500	20	0.69
	Restrictive	15	15	-3.9	-5.0	450	20	0.69

In pressure support ventilation, the set peak inspiratory pressure (PIP)-generated tidal volume of 7–10 ml/kg in the normal model in each body weight with baseline leak. PIP/PEEP was set at 15/5 cm H₂O.

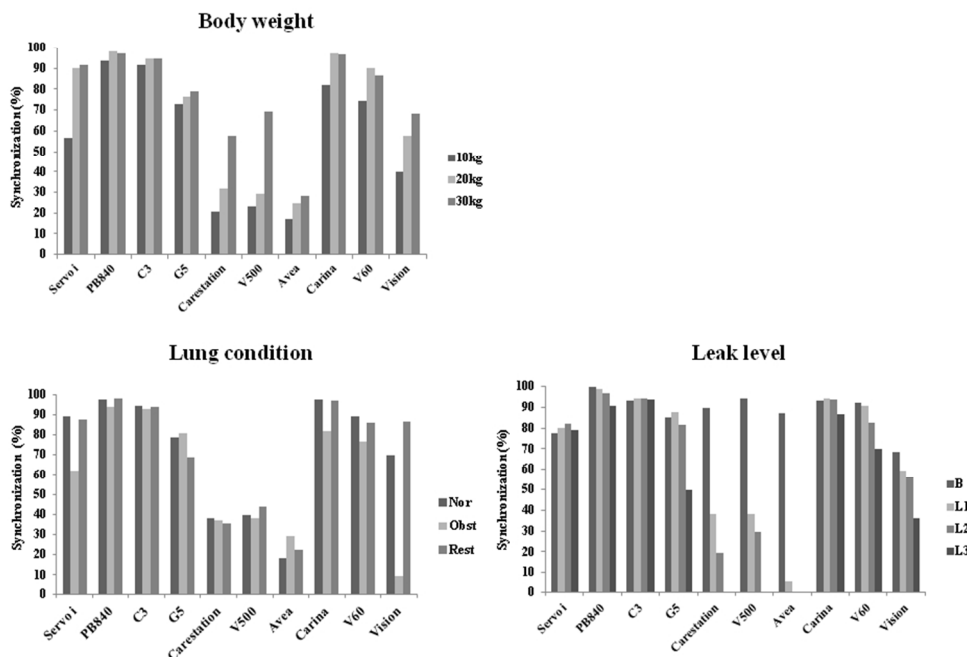
P_{0.1}, negative muscle pressure produced in 100 ms; P_{max}, maximum negative muscle pressure; FRC, functional residual capacity; RR, respiratory rate; I-time, inspiratory time.

Figure 1



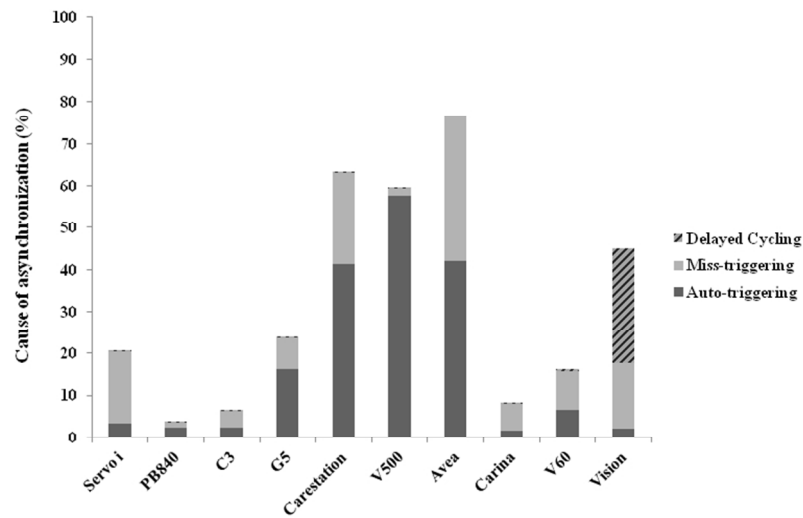
254x190mm (96 x 96 DPI)

Figure 2



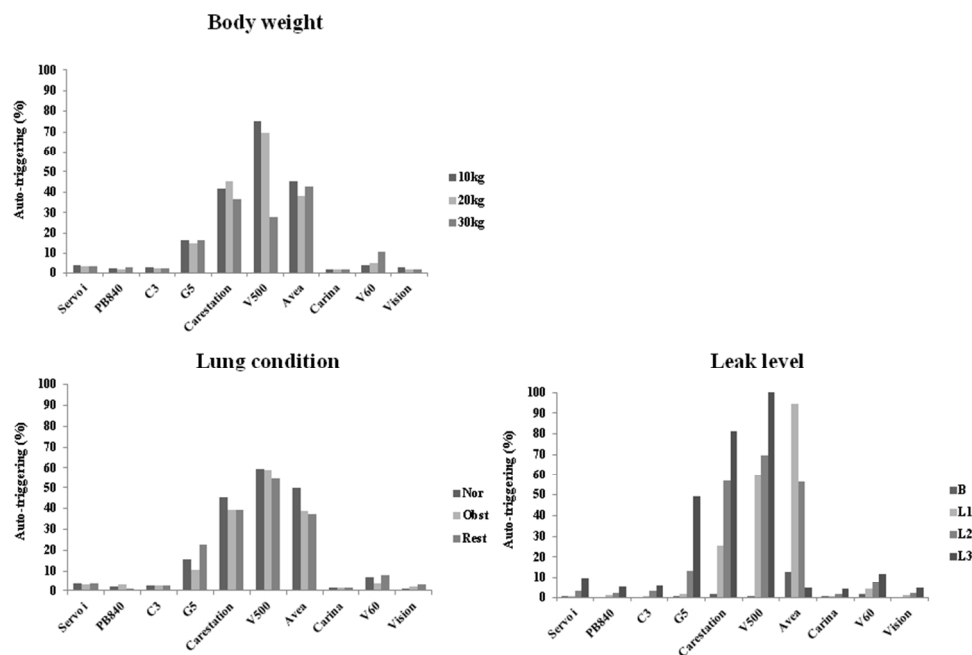
254x190mm (96 x 96 DPI)

Figure 3



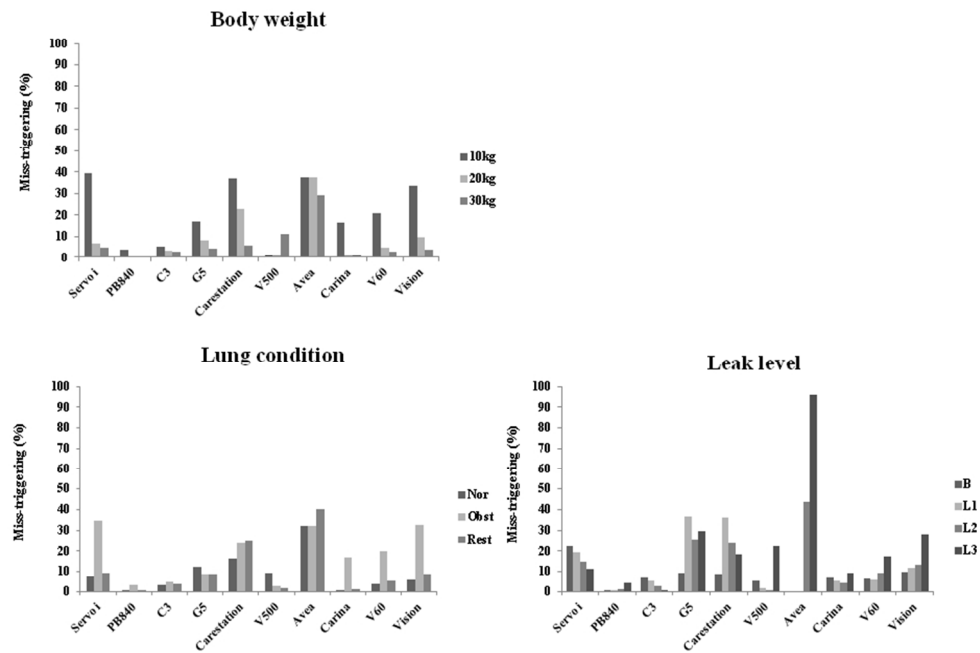
254x190mm (96 x 96 DPI)

Figure 4



254x190mm (96 x 96 DPI)

Figure 5



254x190mm (96 x 96 DPI)